Electronic Supplementary Material (ESI) for Physical Chemistry Chemical Physics.

Supplementary Information:

Nature of the hydrogen-bond-enhanced halogen bonding viewed through electron density changes

Hajime Torii[1,2]*, Akari Kimura[1], and Takanori Sakai[1]

[1] *Applied Chemistry and Biochemical Engineering Course, Department of Engineering, Graduate School of Integrated Science and Technology, Shizuoka University, 3-5-1 Johoku, Naka-ku, Hamamatsu 432-8561, Japan.*

[2] *Department of Optoelectronics and Nanostructure Science, Graduate School of Science and Technology, Shizuoka University, 3-5-1 Johoku, Naka-ku, Hamamatsu 432-8561, Japan.*

* Corresponding author. E-mail: torii.hajime@shizuoka.ac.jp

Computational procedure

Calculations and analyses were carried out for 2-iodophenol at two conformations ($\varphi = 0°$ and 180°) and 2,6-bis(4-ethynyl-3-iodo-*N*-methylpyridinium)-4-fluoroaniline in the bidentate conformation (G2XBme^{2+}-bidentate according to the notation in Refs. S1 and S2), whose structures are shown in Fig. S1. The coordinate system was defined so that (1) for 2-iodophenol, the iodine atom was placed at the origin, the C–I bond was taken along the z axis (C on the $-z$ side), and the molecular plane was placed on the yz plane, and (2) for G2XBme^{2+}-bidentate, the nitrogen atom of the amino group was placed at the origin, the N...F direction was taken along the y axis (F on the $+y$ side), and the H...H direction in the amino group was taken parallel to the z axis. For both molecules, the structure was optimized, and then the electron density and the electrostatic properties were calculated, with the ωB97XD functional[S3,S4] of the density functional theory (DFT) and the def2SVP basis set[S5,S6] using the Gaussian 09 program,[S7] followed by the analyses carried out with our original programs. By using the def2SVP basis set, the relativistic effect is taken into account with the effective core potential for the iodine atom. Additional calculations were also conducted for some related molecules as described below.

The electron density $\rho^{(el)}(\boldsymbol{r})$ was calculated at the evaluation points $\boldsymbol{r}$ taken in a rectangular box of 10.0 × 15.3 × 15.6 Å^3 for 2-iodophenol and 11.8 × 18.2 × 28.6 Å^3 for G2XBme^{2+}-bidentate (determined so that each boundary of the box is at least 5 Å from any atom in the molecule), with the interval of 0.02 Å. Then, the analyses were carried out in the following two ways. First, to clearly see the anisotropic nature of the distribution of the valence electrons on the I atom(s), the electron density calculated for the iodide ion (I^-), which is spherically isotropic, was subtracted from that of each molecule, superimposing the location(s) of the I atom(s), following the procedure developed in the previous studies.[S8,S9] Second, to see the changes in the electronic structural properties induced by the presence of the nearby hydrogen-bond donating group, the electron density difference was calculated between 2-iodophenol and iodobenzene, and between G2XBme^{2+}-bidentate and 1,3-bis(4-ethynyl-3-iodo-*N*-methylpyridinium)-benzene (G1XBme^{2+}-bidentate according to the notation in Refs. S1 and S2). In this case, only the structural parameters related to the substituted atoms (the hydrogen atom substituting the hydroxyl group in 2-iodophenol, and the hydrogen atoms substituting the amino group and the fluorine atom in G2XBme^{2+}-bidentate) were optimized with the locations of the other atoms being fixed.

In addition to these, the first type of calculations was carried out for iodobenzene to check the anisotropy of the electron density on the I atom in the absence of the OH group, and the second type of calculations was carried out for nitrobenzene and benzonitrile to compare the effects of the nature of the functional group attached to the benzene ring on the electron density changes.

For 2-iodophenol, whose structure is simple enough to analyze the electrostatic properties, the electrostatic potential around the molecule was calculated, and was fitted by atomistic models to see the contributions of different parts in the molecule to the electrostatic potential. The evaluation points of the electrostatic potential were taken, similar to the previous studies,[S8,S10,S11] with the interval of 0.4 Å in a

rectangular box of $20 \times 24 \times 30$ Å^3, with the molecule being placed at the center, but the points within 1.6 Å from hydrogen atoms or within 2.8 Å from any other atoms of the molecule were excluded. Then, the following three models developed in the previous studies[S8,S9] were tried: (1) the charge-only model, where electric partial charges are placed only on the atomic sites, (2) the quadrupole model, where an electric quadrupole is placed on the I atom in addition to the electric partial charges on all the atoms, and (3) the extra-point model, where an electric partial charge is placed at the extra point located close to the I atom in addition to the electric partial charges on all the atoms. In this extra-point model, the minimum of the electron density difference of the first type, $\delta[\rho^{(\mathrm{el})}(\boldsymbol{r})] \equiv [\rho^{(\mathrm{el})}(\boldsymbol{r})]_{\mathrm{molecule}} - [\rho^{(\mathrm{el})}(\boldsymbol{r})]_{\mathrm{iodide}}$, on the $z > 0$ side was taken as the location of the extra point. It is found that this location (z = 1.04 Å) is the same among the two conformations of 2-iodophenol [shown in Fig. 1a and b in the main text] and iodobenzene (shown in Fig. S2). The parameters of these models derived from the fitting are shown in Table S1.

As shown in Fig. 2a and b in the main text, the electrostatic potential along the z axis is best reproduced with the extra-point model. As a result, based on this model, the contributions to the electrostatic potential was examined by decomposing the molecule into the following three parts: (i) the (C)–I...EP part, with the full electric partial charges on the I atom and the extra point (EP), and the neutralizing electric charge on the C_2 atom, (ii) the (C)–O–H part, with the full electric partial charges on the OH group and the neutralizing electric charge on the C_1 atom, and (iii) the rest of the molecule, with the full electric partial charges on the C_3, C_4, C_5, and C_6 atoms and the hydrogen atoms bonded to these, and the residual electric charges on the C_1 and C_2 atoms.

References

S1 A. M. S. Riel, D. A. Decato, J. Sun, C. J. Massena, M. J. Jessop and O. B. Berryman, The Intramolecular Hydrogen Bonded–Halogen Bond: A New Strategy for Preorganization and Enhanced Binding. *Chem. Sci.,* 2018, **9**, 5828–5836.

S2 A. M. S. Riel, R. K. Rowe, E. N. Ho, A.-C. C. Carlsson, A. K. Rappé, O. B. Berryman and P. S. Ho, Hydrogen Bond Enhanced Halogen Bonds: A Synergistic Interaction in Chemistry and Biochemistry. *Acc. Chem. Res.,* 2019, **52**, 2870−2880.

S3 J.-D. Chai and M. Head-Gordon, Long-Range Corrected Hybrid Density Functionals with Damped Atom–Atom Dispersion Corrections. *Phys. Chem. Chem. Phys.,* 2008, **10**, 6615–6620.

S4 S. Kozuch and J. M. L. Martin, Halogen Bonds: Benchmarks and Theoretical Analysis. *J. Chem. Theory Comput.,* 2013, **9**, 1918–1931.

S5 F. Weigend and R. Ahlrichs, Balanced Basis Sets of Split Valence, Triple Zeta Valence and Quadruple Zeta Valence Quality for H to Rn: Design and Assessment of Accuracy. *Phys. Chem. Chem. Phys.,* 2005, **7**, 3297–3305.

S6 F. Weigend, Accurate Coulomb-Fitting Basis Sets for H to Rn. *Phys. Chem. Chem. Phys.,* 2006, **8**, 1057–1065.

S7 M. J. Frisch, G. W. Trucks, H. B. Schlegel, G. E. Scuseria, M. A. Robb, J. R. Cheeseman, G. Scalmani, V. Barone, B. Mennucci, G. A. Petersson, H. Nakatsuji, M. Caricato, X. Li, H. P. Hratchian, A. F. Izmaylov, J. Bloino, G. Zheng, J. L. Sonnenberg, M. Hada, M. Ehara, K. Toyota, R. Fukuda, J. Hasegawa, M. Ishida, T. Nakajima, Y. Honda, O. Kitao, H. Nakai, T. Vreven, J. A. Montgomery, Jr., J. E. Peralta, F. Ogliaro, M. Bearpark, J. J. Heyd, E. Brothers, K. N. Kudin, V. N. Staroverov, T. Keith, R. Kobayashi, J. Normand, K. Raghavachari, A. Rendell, J. C. Burant, S. S. Iyengar, J. Tomasi, M. Cossi, N. Rega, J. M. Millam, M. Klene, J. E. Knox, J. B. Cross, V. Bakken, C. Adamo, J. Jaramillo, R. Gomperts, R. E. Stratmann, O. Yazyev, A. J. Austin, R. Cammi, C. Pomelli, J. W. Ochterski, R. L. Martin, K. Morokuma, V. G. Zakrzewski, G. A. Voth, P. Salvador, J. J. Dannenberg, S. Dapprich, A. D. Daniels, Ö. Farkas, J. B. Foresman, J. V. Ortiz, J. Cioslowski and D. J. Fox, *Gaussian 09, Revision D.01*, Gaussian, Inc., Wallingford, CT, 2013.

S8 K. Saito, R. Izumi and H. Torii, Dissecting the Electric Quadrupolar and Polarization Effects Operating in Halogen Bonding through Electron Density Analysis with a Focus on Bromine. *J. Chem. Phys.,* 2020, **153**, 174302.

S9 K. Saito and H. Torii, Hidden Halogen-Bonding Ability of Fluorine Manifesting in the Hydrogen-Bond Configurations of Hydrogen Fluoride. *J. Phys. Chem. B,* 2021, **125**, 11742–11750.

S10 H. Torii, The Role of Atomic Quadrupoles in Intermolecular Electrostatic Interactions of Polar and Nonpolar Molecules. *J. Chem. Phys.,* 2003, **119**, 2192–2198.

S11 H. Torii and M. Yoshida, Properties of Halogen Atoms for Representing Intermolecular Electrostatic Interactions Related to Halogen Bonding and Their Substituent Effects. *J. Comput. Chem.,* 2010, **31**, 107–116.

Supplementary Figures

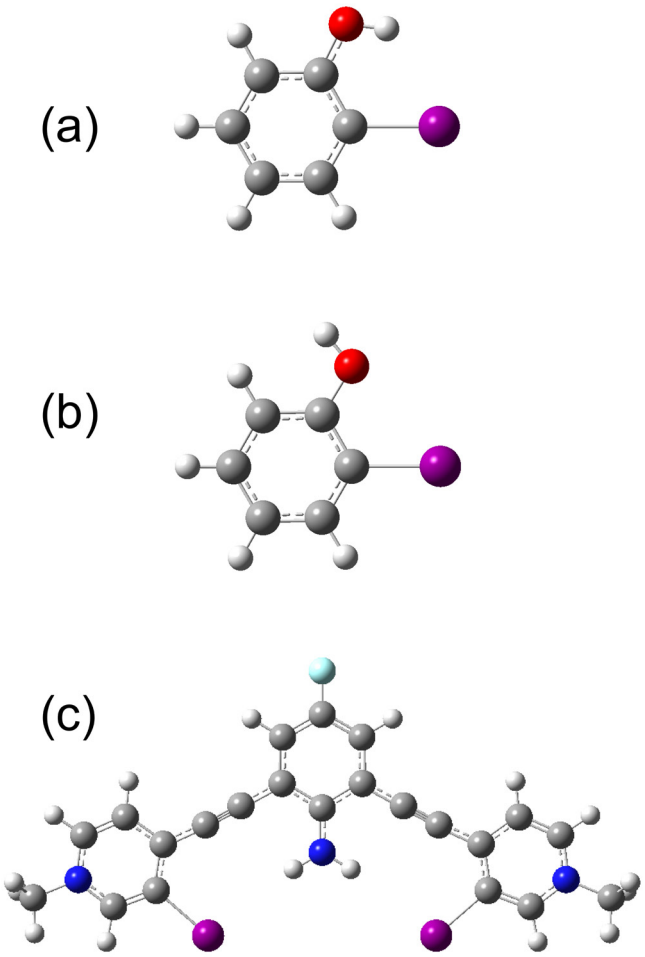

Fig. S1. Structures of (a) 2-iodophenol at $\varphi = 0°$, (b) 2-iodophenol at $\varphi = 180°$, and (c) G2XBme^{2+}-bidentate.

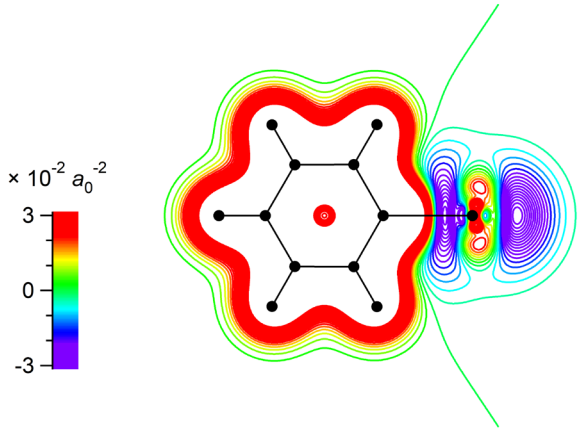

Fig. S2. Two-dimensional contour plot of $\int dx\, \delta[\rho^{(el)}(\boldsymbol{r})]$ [i.e., integration along the x axis of $\rho^{(el)}(\boldsymbol{r})$ calculated in three dimensions $\boldsymbol{r} = (x, y, z)$] calculated at the ωB97XD/def2SVP level for the electron density difference taken between iodobenzene (C_6H_5I) and the iodide ion (I^-), i.e., $\delta[\rho^{(el)}(\boldsymbol{r})] \equiv [\rho^{(el)}(\boldsymbol{r})]_{\text{iodobenzene}} - [\rho^{(el)}(\boldsymbol{r})]_{\text{iodide}}$. The contours in the two-dimensional plot are drawn with the interval of $0.36 \times 10^{-2}\ a_0^{-2}$ in the range from $-9 \times 10^{-2}\ a_0^{-2}$ to $9 \times 10^{-2}\ a_0^{-2}$, with the color code shown on the left-hand side. (Note that the plot is saturated in the spatial region of the benzene ring because the electron density difference is taken with the iodide ion.) The atomic positions are indicated with black filled circles.

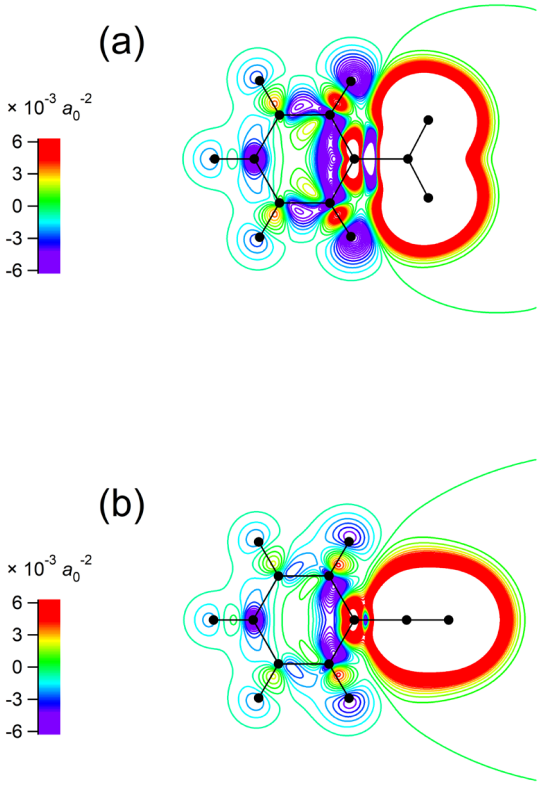

Fig. S3. Two-dimensional contour plots of $\int dx\, \delta[\rho^{(el)}(\boldsymbol{r})]$ calculated at the ωB97XD/def2SVP level for the electron density difference taken between (a) nitrobenzene and benzene, i.e., $\delta[\rho^{(el)}(\boldsymbol{r})] \equiv [\rho^{(el)}(\boldsymbol{r})]_{\text{nitrobenzene}} - [\rho^{(el)}(\boldsymbol{r})]_{\text{benzene}}$, and (b) benzonitrile and benzene, i.e., $\delta[\rho^{(el)}(\boldsymbol{r})] \equiv [\rho^{(el)}(\boldsymbol{r})]_{\text{benzonitrile}} - [\rho^{(el)}(\boldsymbol{r})]_{\text{benzene}}$. The contours in the two-dimensional plots are drawn with the interval of $0.72 \times 10^{-3}\ a_0^{-2}$ in the range from $-18 \times 10^{-3}\ a_0^{-2}$ to $18 \times 10^{-3}\ a_0^{-2}$, with the color code shown on the left-hand side. (Note that each plot is saturated in the spatial region of the nitro or nitrile group because the electron density difference is taken with the benzene molecule.) The atomic positions are indicated with black filled circles.

Supplementary Table

Table S1. The electric partial charges and quadrupole moment obtained from the fitting to the electrostatic potential around 2-iodophenol at two conformations ($\varphi = 0°$ and 180°).

		$\varphi = 0°$			$\varphi = 180°$		
property	atom[a]	charge-only model	quadrupole model	extra-point model	charge-only model	quadrupole model	extra-point model
partial charge / e	C_1	1.1880	0.2331	0.1856	1.3688	0.2566	0.2115
	C_2	–1.1926	–0.0159	0.2487	–1.2407	0.0591	0.3389
	C_3	0.8245	–0.1752	–0.2241	0.8763	–0.2172	–0.2637
	C_4	–0.7929	–0.2439	–0.2575	–0.7955	–0.1697	–0.1865
	C_5	0.4319	–0.0440	–0.0494	0.4445	–0.1051	–0.1110
	C_6	–0.8291	–0.2513	–0.2652	–0.9912	–0.3154	–0.3310
	I	0.1343	–0.0572	–0.5176	0.1397	–0.0703	–0.5711
	O	–0.5836	–0.4442	–0.4313	–0.6999	–0.4662	–0.4563
	H(OH)	0.3231	0.3566	0.3550	0.4195	0.4010	0.4015
	H(C_3)	–0.0307	0.1874	0.2003	–0.0613	0.1717	0.1843
	H(C_4)	0.2261	0.1595	0.1667	0.2250	0.1465	0.1544
	H(C_5)	0.0599	0.1259	0.1303	0.0693	0.1458	0.1506
	H(C_6)	0.2409	0.1692	0.1760	0.2455	0.1632	0.1708
	extra point[b]			0.2827			0.3075
quadrupole / ea_0^2	I		2.5049			2.7312	

[a] The carbon atoms are numbered according to the IUPAC nomenclature.

[b] Located at z = 1.04 Å.